# Detection of wave propagation by a nonstationary cross-spectral density technique

Alfredo A. ORTIZ and Frank K. LU

Aerodynamics Research Center, Mechanical and Aerospace Engineering Department, University of Texas at Arlington, Arlington, Texas 76019-0018, USA

**Abstract**

The accurate determination of the speed of a propagating disturbance is important for a number of applications. A nonstationary cross-spectral density phase technique was developed to provide a statistical estimation for the propagation time, and was applied to a shock and a detonation wave. The results show that by including an envelope signal, the technique is an improvement over the traditional time-of-flight method, but it is more prone to error than the cross-correlation technique.

**Key words**

Wave propagation, Cross-spectrum, Time of flight

## 1. Introduction

Determining the speed of a propagating disturbance is important for a number of applications. In particular, the propagation of a detonation wave is of importance in fundamental studies of detonations as well as in the development of pulse detonation engines [1].

The most common method for determining the wave propagation speed is by the time-of-flight (TOF) method. The average wave propagation speed is defined as

$$\overline{u} = \frac{\Delta x}{\Delta t} \tag{1}$$

where the distance between the sensors is known. This method is the most simplistic approach, but it can lead to poor estimates of uncertainty. The TOF method makes certain assumptions on the detection of the disturbance, primarily, that the disturbance results in a distinct signal. In reality, however, such a signal is subject to some uncertainty due to transducer characteristics, including thermal drift, the medium that the disturbance is propagating through and the data acquisition process itself. To evaluate the uncertainty, a nonstationary cross-spectral density phase (NCSDP) technique was developed. Specifically, this technique was applied to the propagation of shock and detonation waves.

## 2. Determination of the Propagation Time

### 2.1 Non-stationary cross-correlation technique

A propagating disturbance is a nonstationary event. In practice, the nonstationary signal may be influenced by external factors as highlighted above. Previously, a nonstationary cross-correlation (NCC) technique was developed to improve on the time-of-flight technique so as to handle the various external influences [2]. The NCC technique applies four criteria to the data, and computes a time-varying cross-correlation function, yielding a time delay surface. The surface is used to provide a statistical approach to determining the propagation time for the propagating wave through locating the peak in the surface. This time delay is the time-of-flight of Eq. (1). Knowing the transducer distance then allows the propagation speed to be evaluated.

### 2.2 Non-stationary cross-spectral density phase

A spectral method, known as the non-stationary cross-spectral density phase (NCSDP) method, that is based on the cross-correlation function is proposed. The function $W_{xy}(f,t)$ is obtained by a Fourier transform of the discrete NCC as follows:

$$\mathscr{W}_{xy}(f,t) = \int R_{xy}(\tau,t) e^{-j2\pi f\tau} d\tau \tag{2}$$

$$W_{xy}(f,t) = \begin{cases} 2\mathscr{W}_{xy}(f,t) & f > 0 \\ \mathscr{W}_{xy}(f,t) & f = 0 \\ 0 & f < 0 \end{cases}. \tag{3}$$

The one-sided, nonstationary frequency-time cross-spectral density function can then be represented by a real and an imaginary part known as the co- and quad-spectrum respectively. Both functions are shown in the following equations, and are necessary in determining the time delay between the given signals:

$$C_{xy}(f,t) = \frac{1}{2}\left[W_{xy}(f,t) + W_{yx}(f,t)\right] \tag{4}$$

$$C_{xy}(f,t) = \left|W_{xy}(f,t)\right| \cos\theta_{xy}(f,t) \tag{5}$$

$$Q_{xy}(f,t) = \frac{1}{2}\left[W_{xy}(f,t) - W_{yx}(f,t)\right] \tag{6}$$

$$Q_{xy}(f,t) = \left|W_{xy}(f,t)\right| \sin\theta_{xy}(f,t). \tag{7}$$

Using the above relationships, the phase angle can be computed as

$$\theta_{xy}(f,t) = \tan^{-1}\frac{Q_{xy}(f,t)}{C_{xy}(f,t)}. \tag{8}$$

Since the inverse tangent function is bounded, the above equation does not account for the quadrant being computed, thus requiring the phase angle to be shifted to its proper quadrant.

The disturbance is assumed to be nondispersive for the purpose of this study. It is also advisable to restrict the sensor usable bandwidth to less than 10 percent of the natural frequency to avoid introducing phase errors.

2.2.1 *Zoom transform*

The spectral resolution of the signals has to be considered prior to applying the spectral analysis. Since the measurement of a detonation wave requires a high sampling rate with a limited amount of samples before any retonation or reflected wave occurs, the spectral resolution for the signal can be very poor. The poor resolution and the use of a multi-valued function (Eq. (8)) in computing the phase angle leads to an uncertainty of $2n\pi$. So the uncertainty is dependent on how frequent the phase angle jumps with respect to the spectral resolution. This uncertainty can propagate to an incorrect calculation of the time delay for the given signals.

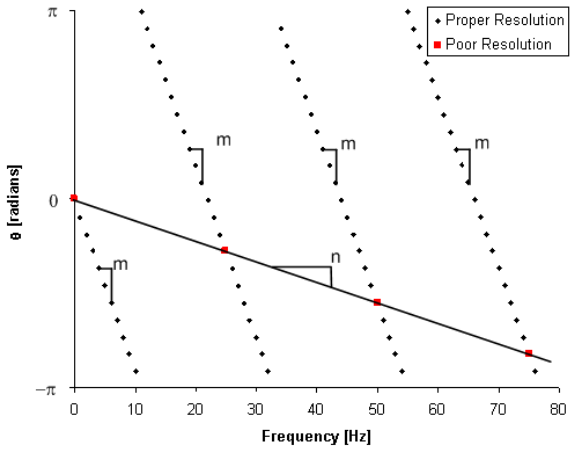


Figure 1 - The effect of poor spectral resolution on determining the phase angle's trend.

An example of a poor and proper resolution is shown in Fig. 1. In the example, the poor resolution is only able to capture one point for each phase jump, which provides an incorrect trend of the phase angle with respect to frequency. The incorrect trend is represented by the slope *n* in Fig. 1. The proper resolution on the other hand will provide several points that are sufficient to generate a proper trend noted by *m* in the figure.

The $2n\pi$ uncertainty can be resolved with a much finer spectral resolution, which requires a larger sample size that is not always possible. An alternative method is to apply a zoom transform to the data series. The zoom transform can improve the spectral resolution, which will provide a better representation of the cross-spectral density phase function. The spectral information lost due to inadequate sample size is minimized, and can be recovered to an acceptable tolerance with the zoom transform. Also, since the wave is assumed to be captured as a nondispersive propagation, the phase angle's linearity with frequency should contain no unexpected phase jumps, allowing for the zoom transform to be applied to limited samples.

2.2.2 *Coherence function*

Another form of uncertainty arises when the coherence function is not unity for the entire spectrum. The coherence function is an indicator of how strong of a correlation there is between the two signals for the entire spectrum. The coherence function is provided by

$$\gamma_{xy}^2(f,t) = \frac{\left|W_{xy}(f,t)\right|^2}{W_{xx}(f,t)W_{yy}(f,t)}. \tag{9}$$

A coherence value of unity for the entire spectrum is the ideal situation; however, it is not always possible to have a strong coherence throughout the spectrum. The nonlinearity relationship between the signals and noise in the signals yield a coherence of less than unity. For this reason, a limiting factor of 50% was applied for rejecting regions of high uncertainty.

2.2.3 *Phase uncertainty*

The phase angle can be determined once the coherence function is known and it is given by

$$\Delta\hat{\phi}_{xy}(f,t) \approx \sin^{-1}\left(\frac{\left[1-\gamma_{xy}^2(f,t)\right]^{1/2}}{\left|\gamma_{xy}(f,t)\right|\sqrt{2n_d}}\right). \tag{10}$$

Referring to the above equation, there are two ways of improving the uncertainty for the phase angle. One way is to ensure that both signals are highly coherent, and the next is to have a large number of averages. It should also be noted that with a low coherence value, the uncertainty in the phase angle becomes very large which then requires a large ensemble of averages to reduce the uncertainty to a tolerable level. For this reason, a coherence limit of 50% is applied to the NCSDP function. While this is somewhat arbitrary, it allows for an adequate tolerance with an adequate ensemble of averages for the NCSDP function. Further information about the uncertainty of the phase angle is provided in [3].

2.2.4 *Weighting function*

Misrepresentation of the phase uncertainty can also arise if a weighting function is not applied to the NCC function. The error due to spectral leakage would propagate to the coherence function and the uncertainty in the phase estimate. Based on unreported work, a Blackman-Harris window was selected as the weighting function as it provides a relatively higher coherence than the typical Hanning and Hamming window.

2.2.5 *Unwrap phase*

After application of the previous methods for reducing the uncertainty in the phase angle, a weighted-resetting unwrap of the phase angle is utilized to reduce the uncertainty for the trend of the phase angle. The unwrapping of the phase angle is used to remove the discontinuity in the phase jumps, which provides a smooth and continuous representation of the phase angle by the addition or subtraction of a multiple of $2\pi$ to the phase angle. This method consists of several unwrapped portions of the phase angle. The phase angle is unwrapped till the coherence limit is crossed, and then

determines the slope of the unwrapped phase. The process would continue till the entire data set is processed. Afterwards, a weighted percentage dependent on the amount of samples for a given trend is applied and used to compute an overall trend for the phase angle with respect to frequency. This method has the advantage that the uncertainty produced by the coherence is limited further by resetting the phase angle, and by weighting the larger portions of values above the 50% limit heavier. A problem arises if the coherence for the signals is constantly crossing the coherence limit, which will provide small sample sets for determining the slope. As the sample size approaches one for a given set, the estimation for the trend decreases. For sample sets consisting of a sample size of 1, a discarding of the data set is necessary since it is an inadequate amount for determining a trend.

The above method is not the only one that can be applied, but is the one currently implemented for improving the estimation of the trend. Two other methods that can be used are not to unwrap the phase, and to have the signal unwrapped once. The advantage to the wrapped phase angle is that it is less computationally intensive, and it will produce a large dataset of slopes to improve the averaging process. A problem that can arise from this method is that it may contain a few points before a phase jump, which may lead to poor estimates of the trend of the phase angle. This problem may be overcome by a finer spectral resolution that will then require more computations with a zoom transform.

The last method would consist of one trend per time frame. The advantage to this method is that is uses a large amount of samples to determine a single trend, which may reduce the error for the phase. However, further error in unwrapping the phase may propagate if large portions of coherence limit crossing occur. This method is not recommended due to the uncertainty propagating with increasing frequency that is introduced from poorly coherent signals.

2.2.6 *Linear fit*

After unwrapping the phase, a linear least squares fit (LLSF) method was applied for determining the slope. No weighting scheme was applied in the determination of the linear fit.

For this method, the time delay is not directly proportional to the phase of the NCSDP function due to the application of the FFT to the data. The discrete nature as well as spectral leakage contributes to the inability of the FFT to compute the Fourier transform of the NCC function. This is clearly seen when the FFT of the autocorrelation function for both signals include imaginary components. It should be noted that even functions, such as the autocorrelation function, contain no imaginary components after the application of the Fourier transform.

Since the autospectral density functions have a phase angle, differences between the theory and application have to be determined. An example of an unwrapped phase angle for the autospectral and cross-spectral density function at a given time step for a detonation wave is shown in Fig. 2. The figure shows the small phase difference between the two functions, where the phase for the autospectrum is the reference line for no time delay.

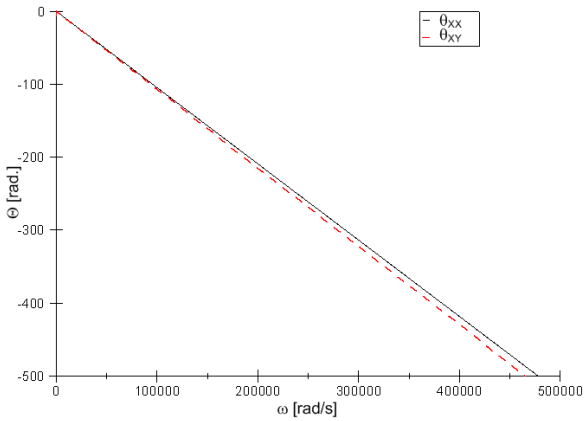


Figure 2 - The unwrapped phase angle for the autospectral (solid black line) and cross-spectral density function (dashed red line) for a given time step.

It can be shown that

$$\theta_{xy}(\omega,t) = -\left(\tau_{xy} + \frac{N-1}{f_s}\right)\omega . \qquad (11)$$

The time delay can be computed by setting the terms in the parenthesis in Eq. (11) to be equal to the slope determined from the LLSF method. Equation (11) can also be used for the autospectral density phase angle. Obviously, there is no time delay for the autospectrum.

An alternative method for determining the time delay is to compute the average difference between the autospectrum and cross-spectrum. This method does not require knowledge of the sampling properties and is given by

$$\overline{\tau}_{xy}(t) = \frac{\left(\left.\frac{d\theta}{d\omega}\right|_{xx} - \left.\frac{d\theta}{d\omega}\right|_{xy}\right) + \left(\left.\frac{d\theta}{d\omega}\right|_{yy} - \left.\frac{d\theta}{d\omega}\right|_{xy}\right)}{2} . \qquad (12)$$

The time delay estimate would then be determined by ensemble averaging over time. Chauvenet's criterion for each time step was then applied to eliminate outliers, specifically near the disturbance.

2.2.7 *Envelope correlation coefficient*

An alternate method for improving the estimate of the propagation time is known as the envelope correlation coefficient [4]. This method utilizes the squared envelope for correlation, which provides a sharper and more definitive estimation of the propagation time. The derivation for the envelope correlation coefficient is shown in detail [4] and is represented as

$$\rho_{uv}(t_i,\tau_j) = \rho_{xy}(t_i,\tau_j) + \tilde{\rho}_{xy}(t_i,\tau_j) \qquad (13)$$

where the coefficients are given by

$$\rho_{xy} = \frac{R_{xy}\left(t_i,\tau_j\right)}{\sqrt{\left[R_{xx}\left(t_i,0\right)+\left(\bar{x}\right)^2\right]\left[R_{yy}\left(t_i,0\right)+\left(\bar{y}\right)^2\right]}} \quad (14)$$

$$\tilde{\rho}_{xy} = H\left[\rho_{xy}\right]. \quad (15)$$

The NCC method was modified to compute the cross-correlation coefficient function as well as the Hilbert transformation of the coefficient, which are used to define the envelope correlation coefficient. Similar to the original NCC method, the modified version can be applied to the NCSDP to provide an improved estimate of the propagation time.

## 3. Results

### 3.1 Application to a shock tube experiment

The NCSDP method was applied to determine the wave propagation for the incident and reflected shock waves for a closed-end shock tube. A set of pressure profiles for the experiment is provided in Fig. 3.

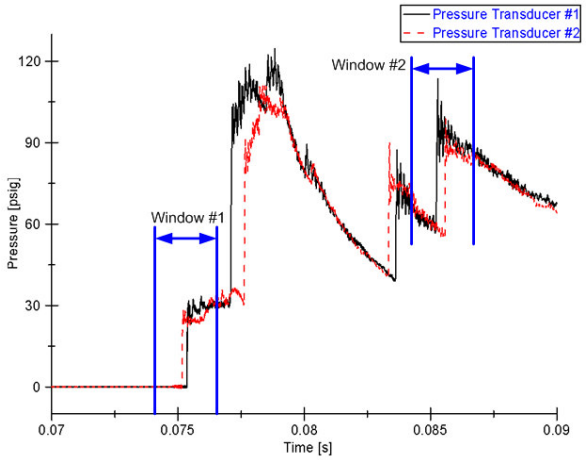


Figure 3 – The pressure profile for a closed-end shock tube experiment containing the incident and reflected shock waves.

The result from applying the NCC is shown in Fig. 4. The peak value for the NCC symbolizes the most probable time delay of the given signal, which defines the propagation time for the shock wave.

The results from the NCC are then used to compute the NCSDP, and a comparison for the results is provided in Tables 1 and 2. Comparing the NCC with the NCSDP, it is clearly seen that the NCSDP yields a larger uncertainty in the determination of the propagation time. The large uncertainty provided with the NCSDP method is due to poor coherence in the signals. Referring to Fig. 5, the coherence function for the incident shock is extremely poor as it contains a large percentage of frequencies below the coherence limit, leading to a large error in the determination of the phase. Similar results are also seen for the reflected shock wave that contains a higher coherence between the transducers, but still has a large percentage below the coherence limit.

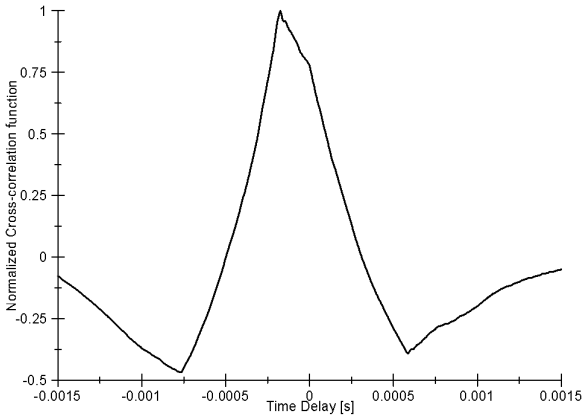


Figure 4 – The normalized cross-correlation function for the incident shock wave.

Table 1 – Propagation time results for the incident shock wave.

| | τ [ms] | σ [ms] |
|---|---|---|
| TOF | -0.178 | - |
| NCC - Raw Data | -0.165 | 0.087 |
| NCC - Envelope Signal | -0.186 | 0.033 |
| NCSDP - Raw data | 0.095 | 0.274 |
| NCSDP - Envelope Signal | -0.161 | 0.032 |

Table 2 – Propagation time results for the reflected shock wave.

| | τ [ms] | σ [ms] |
|---|---|---|
| TOF | 0.316 | – |
| NCC - Raw Data | 0.313 | 0.002 |
| NCC - Envelope Signal | 0.335 | 0.003 |
| NCSDP - Raw data | 0.239 | 0.101 |
| NCSDP - Envelope Signal | 0.318 | 0.030 |

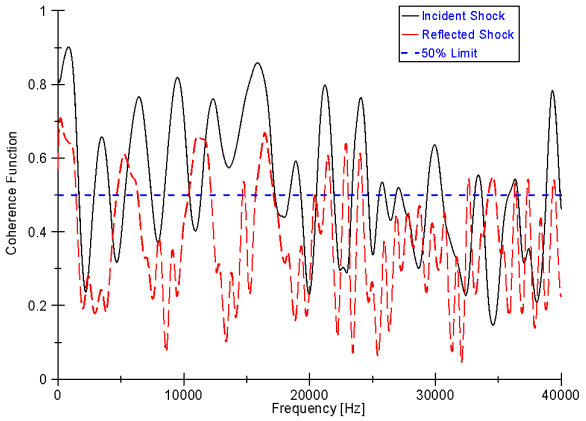


Figure 5 – The coherence function for the incident and reflected shock wave.

The uncertainty can further be reduced for these techniques if envelope functions were applied to the raw data first. The results for both the NCC and NCSDP

methods where the squared envelopes were used are also displayed in Tables 1 and 2. A significant improvement of the estimate and uncertainty for the propagation time is clearly seen for both methods. The NCC for the envelope signals is shown in Fig. 6. It is clearly seen that the envelope signals improves the time delay determination (in comparison to the un-enveloped approach displayed in Fig. 4), and minimizes the error introduced due to the bias nature of the finite window. The cross-correlation is biased for values surrounding no time delay, and appears as an attenuation toward values near the edges of the window.

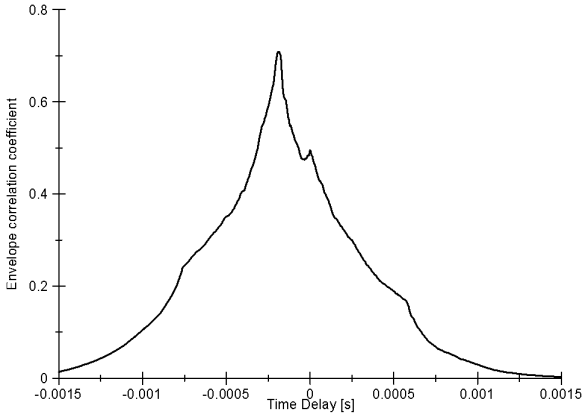


Figure 6 – The cross-correlation function for the envelope signals of the incident shock wave.

### 3.2 Application to a propagating detonation wave

Data from a propagating detonation wave was also analyzed with the NCSDP method. The pressure profiles for six transducers that are separated by four inches on a PDE are shown in Fig. 7. The PDE used for this study was 1" in diameter, and used a low-energy spark plug to ignite the Propane-Oxygen mixture. The NCC for the given pressure transducers as well as the NCC for the envelope signals are provided in Figs. 8 and 9. These results once again were used to determine the NCSDP, and the results for each method are displayed in Tables 3 and 4 for a series of transducers. Similar to the results from the shock tube, the uncertainty for the NCSDP is larger than the NCC method. The estimation of the propagation time is also highly influenced by the violent pressure oscillations as seen in Fig. 7. The oscillations are especially troublesome for transducers 4 and 5, which did not properly resolve the shock front.

The oscillations are thought to be due to a combination of retonations, reflected shock waves, and the recession of the pressure transducers. The recession of the transducers allows for the phenomenon known as Helmholtz resonance to occur. It can be shown that the resonant frequency is a function of the dimensions of the cavity as well as the speed of sound. Since it is assumed that the cavity is the same dimensions for all the transducers, the frequency of the oscillations is then determined by the speed of sound. So an increase in temperature will increase the frequency of the oscillations. These oscillations provide additional correlated peaks in the NCC method as shown in Fig. 8. Unfortunately these additional correlated peaks influence the phase to some form of phase averaging that produces inaccurate results of the propagation time.

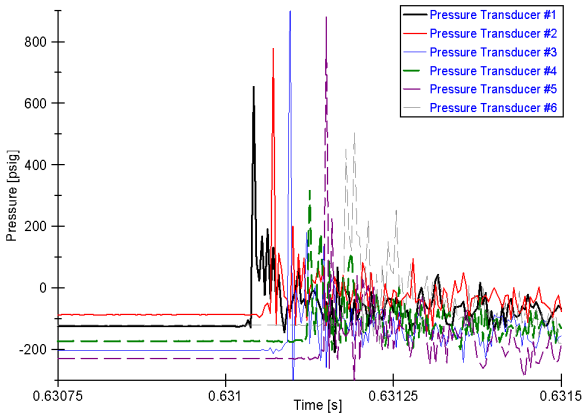


Figure 7 – The pressure profile for a set of pressure transducers for a PDE.

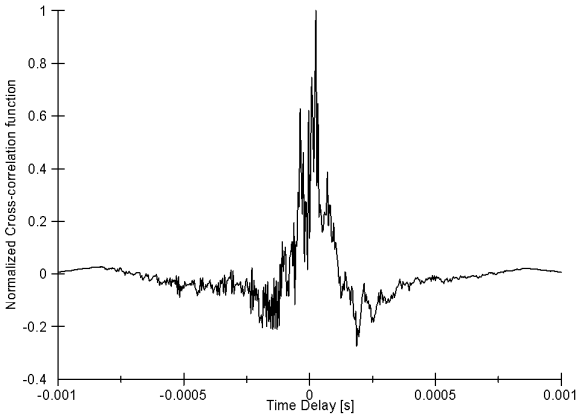


Figure 8 – The normalized cross-correlation function for pressure transducers 4 and 5.

Table 3 – Propagation time results for the PDE with the use of the NCSDP method.

| Sensor | Raw Data | | Envelope Signal | | TOF |
|---|---|---|---|---|---|
| # | τ [μs] | σ [μs] | τ [μs] | σ [μs] | τ [μs] |
| 1,2 | 29.8 | 0.4 | 29.2 | 0.1 | 29.2 |
| 2,3 | 22.9 | 0.6 | 25.3 | 0.1 | 25.0 |
| 3,4 | 75.3 | 9.5 | 27.5 | 0.2 | 29.2 |
| 4,5 | -10.7 | 12.6 | 29.0 | 0.1 | 25.0 |
| 5,6 | 47.6 | 13.1 | 27.0 | 0.1 | 29.2 |
| 1,3 | 50.9 | 7.3 | 54.3 | 0.1 | 54.2 |
| 2,5 | 79.5 | 3.6 | 78.8 | 0.0 | 79.2 |
| 3,5 | 57.1 | 0.6 | 53.7 | 0.2 | 54.2 |

Table 4 – Propagation time results for the PDE with the use of the NCC method.

| Sensor | Raw Data | | Envelope Signal | |
|---|---|---|---|---|
| # | τ [μs] | σ [μs] | τ [μs] | σ [μs] |
| 1,2 | 29.2 | 0.0 | 29.2 | 0.0 |
| 2,3 | 25.0 | 0.0 | 25.0 | 0.0 |
| 3,4 | 29.2 | 0.0 | 29.2 | 0.0 |
| 4,5 | 25.0 | 0.0 | 25.0 | 0.0 |
| 5,6 | 29.2 | 0.0 | 29.2 | 0.0 |
| 1,3 | 54.2 | 0.0 | 54.2 | 0.0 |
| 2,5 | 79.2 | 0.0 | 79.2 | 0.0 |
| 3,5 | 54.2 | 0.0 | 54.2 | 0.0 |

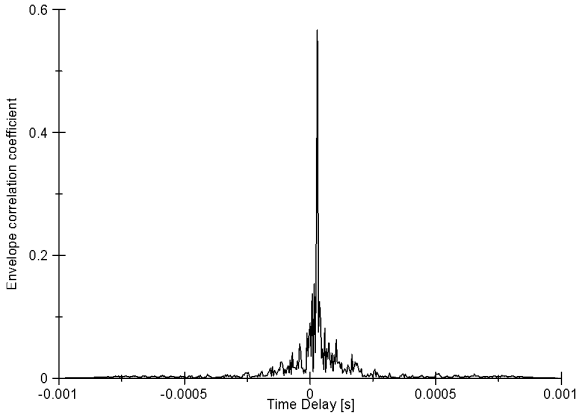


Figure 9 – The cross-correlation function for the envelope signals of pressure transducers 1 and 2.

## 4. Conclusion

The NCSDP method preprocessing of the data by an envelope function appears superior to the TOF method as it provides a statistical means for defining the propagation time for the propagating wave. Unfortunately the NCSDP method yields a larger uncertainty than the NCC due to poorly coherent signals or other physical phenomenon such as Helmholtz resonance. The method is also more computationally intensive than the NCC.

However, the results for the NCSDP may provide additional insight to the current state of the detonation wave for a given set of transducers that is not easily determined with the NCC. Since the NCSDP provides some form of a mean propagation time, it can be compared to the NCC propagation time to determine if the detonation wave has accelerated or decelerated within the given sensors. Further research to the significance of the difference between these methods needs to be done to quantify the results.

## Nomenclature

$C_{xy}$ Co-spectrum
$f_s$ Sampling rate
$H[\ ]$ Hilbert transform
$n_d$ Number of averages
$N$ Sample size
$Q_{xy}$ Quad-spectrum
$R_{xy}$ Nonstationary cross-correlation function
$\overline{u}$ Average wave propagation speed
$W_{xy}$ One-sided frequency-time cross-spectral density
$\mathscr{W}_{xy}$ Double-sided frequency-time cross-spectral density
$\tilde{x}$ Hilbert transformation of $x$
$\Delta t$ Time-of-flight of a disturbance between two sensors
$\Delta x$ Distance between two sensors
$\rho_{xy}$ Nonstationary cross-correlation coefficient function
$\rho_{uv}$ Envelope correlation coefficient function
$\theta_{xy}$ Phase angle
$\gamma_{xy}$ Coherence function
$\tau_{xy}$ Time delay
$\sigma$ Standard deviation
$\omega_n$ Natural frequency
^ Estimate

## Acknowledgements

This work is partly funded by the National University of Singapore via Research Collaboration Agreement No. TL/AE/2008/01.

## References

[1] Li, J., Lai, W.H., Chung, K. and Lu, F.K.: *Uncertainty analysis of deflagration-to-detonation run-up distance*, Shock Waves, Vol. 14, Issue 5-6, (2005), 413-420.

[2] Lu, F.K. and Kim, C.H.: *Detection of wave propagation by cross correlation*, Proceedings of the 38th Aerospace Sciences Meeting and Exhibit, AIAA Paper 2000-0676, (2000).

[3] Bendat, J.S. and Piersol, A.G.: *Engineering Applications of Correlation and Spectral Analysis*, 2nd ed., John Wiley & Sons, Inc., New York, (1993), 309-310.

[4] Bendat, J.S. and Piersol, A.G.: *Random Data Analysis and Measurement Procedures*, 3rd ed., John Wiley & Sons, Inc., New York, (2000), 543-547.